KAWASAKI STEEL TECHNICAL REPORT
No.18 ( May 1988 )

# Burden Distribution Model Experiment in Ferro-Manganese Smelting Furnace with Cardan Type Bell-less Top

Yukio Konishi, Seiji Taguchi, Tsuyoshi Fukutake, Katuyoshi Fukami, Hiroshi Itaya, Yasunori Serizawa

Synopsis :
Cardan type bell-less top with double hoppers located vertically on the furnace axis was applied to ferromanganese smelting furnace(SF) for the sake of good burden-distribution controllability and its durability against high top gas temperature. The burden distribution characteristics were examined with a small scale model apparatus before the start of operation to understand the new system. In the model tests, a similarity condition was firstly investigated, and then ten proper tilting angles of the distributing chute for SF operation were determined within the range of 8° to 26( and the burden distribution characteristics of the apparatus were clarified as that the burden movement in the layer surface toward the furnace center was small and the size segregation scarcely occurred at the time of changing. The results were also confirmed in the test at the furnace filling. The application of results of the model experiment and filling test contributed to stable SF operation.



The body can be viewed from the next page.

# Burden Distribution Model Experiment in Ferro-Manganese Smelting Furnace with Cardan Type Bell-less Top*


Yukio Konishi
Senior Researcher, Ironmaking Lab., I & S Research Labs.

Seiji Taguchi
Senior Researcher, Ironmaking Lab., I & S Research Labs.

Tsuyoshi Fukutake
Dr., Engi., Staff Assistant General Manager, Research Planning Dept., Technical Research Div.

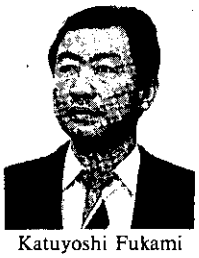

Katuyoshi Fukami
Manager, Technical Sec., Mizushima Works, Kawatetsu Mining Corp.

Hiroshi Itaya
Senior Researcher, Ironmaking Lab., I & S Research Labs.

Yasunori Serizawa
Staff Manager, Iron- & Steelmaking Technology Sec., Steel Plant Engineering Dept.



***Synopsis:***

*Cardan type bell-less top with double hoppers located vertically on the furnace axis was applied to ferromanganese smelting furnace (SF) for the sake of good burden-distribution controllability and its durability against high top gas temperature. The burden distribution characteristics were examined with a small scale model apparatus before the start of operation to understand the new system. In the model tests, a similarity condition was firstly investigated, and then ten proper tilting angles of the distributing chute for SF operation were determined within the range of 8° to 26° and the burden distribution characteristics of the apparatus were clarified as that the burden movement in the layer surface toward the furnace center was small and the size segregation scarcely occurred at the time of charging. The results were also confirmed in the test at the furnace filling. The application of results of the model experiment and filling test contributed to stable SF operation.*


## 1 Introduction

The smelting furnace (SF) at Mizushima Ferro-Alloy Co., Ltd. is a shaft-type furnace for manufacturing ferro-manganese and has a furnace volume of 398 $m^3$ [1]. A Cardan-type bell-less charging apparatus[2], jointly developed by Ishikawajima-Harima Heavy Industries, Paul Wurth (PW) S.A. and Kawasaki Steel, is installed at the smelting furnace. In the PW-Type bell-less charging apparatus, a semi-cylindrical trough-like distribution chute is rotated by gears, while in the Cardan type, a tapered cylindrical chute oscillates in two orthogonal directions of the rotary-axes, giving a circular motion to the chute. Further, the PW-type bell-less top is usually provided with two furnace top bunkers in parallel in the horizontal direction, while in the Cardan type, upper and lower hoppers are provided vertically in a series arrangement, in line with the central axis of the furnace. These are the main differences between the conventional PW apparatus and the Cardan type. A new drive mechanism and distribution chute used with the Cardan type improves the distribution characteristics of charged materials and the durability of the distribution apparatus under high top gas temperature conditions and lowers operating costs.

The present case was the first use of the Cardan type by a Kawasaki group company. Although Kawasaki Steel had experience with the PW-type bell-less top, the motion of material in the distribution chute of the Cardan type is different. Thus, prior to introduction, a small model was constructed and used in experimental investigations of the burden distribution characteristics of the Cardan type apparatus. At the time of filling, investiga-

* Originally published in *Kawasaki Steel Giho*, **19**(1987)2, pp. 80–86

tions, including in-furnace sampling, were also conducted to confirm the validity of the results of the model experiment. An outline of these experiments is given below.

## 2 Features of Cardan Type Bell-less Top

### 2.1 Drive Mechanism

A schematic diagram of the drive mechanism is shown in **Fig. 1**. The distribution chute is secured to a frame which oscillates within a certain range around its own rotary axis (X-axis) so that the chute can swing around the Y-axis, which is perpendicular to the X-axis. The chute starts its swinging motion at the fixed intersection point of the X- and Y-axes. This motion combines rotation of the oscillating frame and a swinging motion centered around a pin and effected by the link in the oscillation frame. The oscillating frame and link are set in motion by the rotation of the power transmission shaft, which has a bend point. The angle of inclination, $\theta$, of the distribution chute can be changed by adjusting the tilting cylinder.

These tilting and rotating motions can be given to the chute independently or simultaneously, permitting free distribution of materials at any position on the burden top.

### 2.2 Features

The Cardan-type charging apparatus has the following features:

(1) The drive mechanism is simple.

(2) Since the main drive unit is outside the furnace, good durability under high top gas temperature conditions can be obtained.

(3) The water-cooled drive unit can be easily manufactured and allows lower operating costs related to cooling than do gas cooling units.

(4) With each turn of the distribution chute, the fixed point of the chute inner surface rotates over 360°C of a circular cross section, and thus the wear of the chute inner surface liner is uniform and liner life is extended, reducing the frequency of linear changes.

These features are especially advantageous for the smelting furnace operation, because the burden top temperature is high.

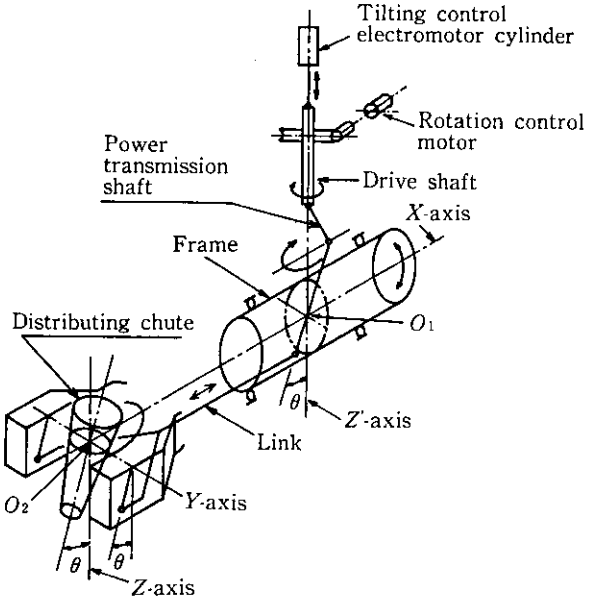


Fig. 1 Drive mechanism

## 3 Small-Scale Model Experiment

### 3.1 Similarity Conditions Necessary for Small-Scale Model Experiment

Reproducing the processes of burden descent and gas flow in a full size blast furnace, and altering conditions for experimental purposes is a costly, time-consuming task. In the present case, widely modified test conditions were required; therefore, a model appratus with a reduced scale of 1/7.5 was devised. The small-scale model and its similarity conditions are described below.

As shown in **Fig. 2**, the trajectory of a falling particle flying at a initial velocity of $V_L$ from a chute having an angle of inclination of $\theta$ is given by Eq. (1).

$$Y = X \cot\theta + \frac{gX^2}{2V_L^2}\sin^2\theta \cdots\cdots\cdots\cdots (1)$$

When the length of the model chute is denoted by $L^*$ and the chute length of the full scale furnace by $L$, Eq (2) gives the similarity condition for trajectory in the space of a reduced scale ratio in which $S = L^*/L$.

$$SY = SX \cot\theta + \frac{g(SX)^2}{2(V_L^*)^2}\sin^2\theta \cdots\cdots\cdots (2)$$

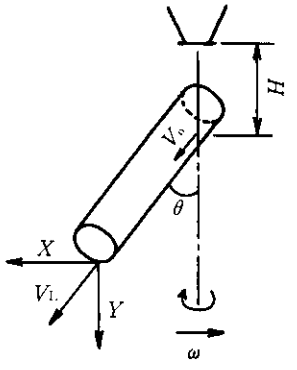


Fig. 2 Explanation of variables used in equations that describe particle motion

Therefore, velocity $V_L^*$, at which a particle flies from the chute tip in the small-scale model experiment, must satisfy Eq. (3).

$$V_L^* = V_L\sqrt{S} \quad \cdots\cdots(3)$$

On the other hand, the motion of a point mass ($m$) on a chute which rotates at a velocity of $\vec{\omega}$ is given by the following equation in the coordinate system $\vec{r} = (r, \theta)$, which rotates at the same velocity.[3]

$$m\frac{d^2\vec{r}}{dt^2} = m\vec{g} - m[\vec{\omega} \times (\vec{\omega} \times \vec{r})] - 2m\left(\vec{\omega} \times \frac{d\vec{r}}{dt}\right) - \vec{R} - \mu|\vec{R}| \times \frac{\frac{d\vec{r}}{dt}}{\left|\frac{d\vec{r}}{dt}\right|} \quad \cdots\cdots(4)$$

The 1st through 5th terms on the right of Eq. (4) represent gravity, centrifugal force, Corioli's force, vertical reaction force from the chute surface, and the frictional force of the chute surface, respectively, and $\mu$ and $t$ are a friction coefficient and time.

In the present apparatus, the inner surface of the chute is of conical shape with a inclination angle of 3° towards the chute tip, approximating a true circular cylinder. Considering the fact that the motion in the cross section perpendicular to the cylinder, which is derived by Corioli's force in Eq. (4), will not exercise a significant effect on motion in the longitudinal direction of the chute, motion in the longitudinal direction of the chute can be calculated using Eq. (5).

$$m\frac{d^2r}{dt^2} = mg\cos\theta + m\omega^2 r\sin^2\theta - m\mu\sin\theta(g - \omega^2 r\cos\theta) \quad \cdots\cdots(5)$$

Assuming that initial velocity at $r = 0$ is $V_0$, velocity $V_L$, when a point mass reaches the chute tip (length $L$), is given by Eq. (6), which is obtained by integrating Eq. (5).

$$V_L = [\omega^2\sin\theta(\sin\theta - \mu\cos\theta)L^2 + 2g(\cos\theta - \mu\sin\theta)L + V_0^2]^{1/2} \cdots(6)$$

Similarly, velocity $V_L^*$ at the chute tip of the model is given by the following Eq. (7), where the chute length is denoted by $L^*$, initial velocity by $V_0^*$, and chute rotation velocity by $\omega^*$:

$$V_L^* = [(\omega^*)^2\sin\theta(\sin\theta - \mu\cos\theta)(L^*)^2 + 2g(\cos\theta - \mu\sin\theta)L^* + (V_0^*)^2]^{1/2} \cdots(7)$$

In order to ensure the similarity of the trajectory of a point mass being discharged from the chute tip, Eq. (3) must be satisfied, as mentioned earlier. Therefore, Eqs. (6) and (7) are substituted into Eq. (3) to obtain Eq. (8).

$$[\omega^2 L - (\omega^*)^2 L^*]\sin\theta LL^* + V_0^2 L^* - (V_0^*)^2 L = 0 \cdots(8)$$

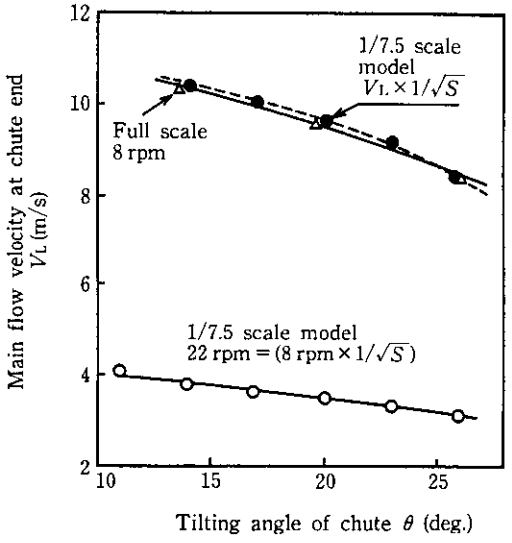


Fig. 3 Effect of tilting angle of chute on main flow velocity at chute end

To satisfy the condition that Eq. (8) is valid at an arbitrarily reduced scale ratio, Eqs. (9) and (10) must be satisfied. The similarity conditions are expressed by Eqs. (9) and (10).

$$\omega^2 L = (\omega^*)^2 L^*, \quad \therefore \frac{\omega^*}{\omega} = \sqrt{\frac{L}{L^*}} = \frac{1}{\sqrt{S}} \quad \cdots\cdots(9)$$

$$V_0^2 L^* = (V_0^*)^2 L, \quad \therefore \frac{V_0^*}{V_0} = \sqrt{\frac{L^*}{L}} = \sqrt{S} \quad \cdots(10)$$

Here, initial velocity $V_0$ at $r = 0$ on the chute is given by Eq. (11), and if $H^*/H = S$ is maintained, $V_0^*/V_0 = S$ will be obtained. Thus, if hoppers are installed at heights corresponding to the reduced-scale ratio, Eq. (11) will be satisfied.

$$V_0 = \sqrt{2gH} \times \cos\theta \quad \cdots\cdots(11)$$

**Figure 3** shows a comparison between the velocity obtained by multiplying the observed velocity at the chute tip in the model experiment and the velocity calculated on the basis of the trajectory of falling burden measured in the actual furnace during filling. The two show good agreement, indicating that the similarity conditions were valid.

### 3.2 Experimental Apparatus

A sketch of the model apparatus is shown in **Fig. 4**. The dimensions of the apparatus were all reduced to a scale of 1/7.5. The furnace has a glazed front surface, and is of the half-cut split type with a throat diameter of 640 mm$\phi$. To lower the stock line, the burden is discharged from the furnace bottom by a solenoid feeder. In the experiment, air was blown in from tuyeres, and

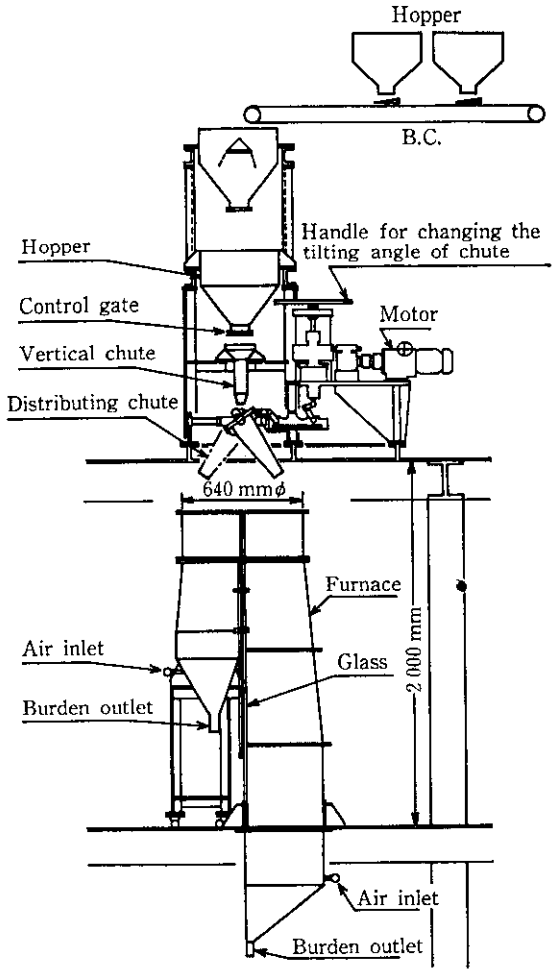


Fig. 4 Experimental apparatus

Table 1 Experimental conditions

| | Item | Full scale | Model*1 |
|---|---|---|---|
| Measurement of falling trajectory | Mean size $D_p$ | | |
| | Coke (mm) | 44.5 | 5.93*2 |
| | Ore (mm) | 28.0 | 3.73*2 |
| | Rotation speed $N_W$ (rpm) | 8 | 22*3 |
| | Discharge speed $W_g$ | | |
| | Coke (kg/s) | 46.7 | 0.304*4 |
| | Ore (kg/s) | 51.3 | 0.335*4 |
| | Tilting angle $\theta$ (°) | — | 32~8 |
| Charging test | Rotating number $R_v$ | 10 | 10 |
| | Charging weight | | |
| | Coke base (t/charge) | 3.5 | 0.0083*5 |
| | Ore/coke | 1.10 | 1.10 |
| | Gas volume $V$ (Nm³/min) | — | 1.15 |

*1 $S=1/7.5$
*2 $D_P^*=D_P\times S$
*3 $N_W^*=N_W\times 1/\sqrt{S}$
*4 $W_g^*=\text{C.B.}\times S^3/(60\times R_v/N_W^*)$
*5 $\text{C.B.}^*=\text{C.B.}\times S^3$

the effect of gas flow on burden distribution was evaluated.

### 3.3 Experimental Conditions and Experimental Method

Major experimental conditions are shown in **Table 1**. The conditions of the model experiment were determined by the previously mentioned scale ratio conditions based on those in the actual furnace. The trajectory of falling burden was measured by feeding a burden from the distribution chute at three different heights into a vessel partitioned at intervals and then measuring the respective weights of the burden as received. From these measurements, values of cumulative weight fraction $F$ from the wall at the respective heights were obtained, and by linking positions at which the $F$ values were constant, the trajectory was determined. In the following, the position at which $F = 50\%$ is called the "trajectory of the main flow."

In the burden distribution experiment at the furnace top, first the surface angle of the levelling coke layer was adjusted to 30°. Next, coke and ore were charged in a series C↓, O↓. In one experiment, this procedure was repeated three times. Prior to charging, the burden was discharged from the bottom of the furnace to adjust the stock-line. At the third charge of coke and ore, measurements of the burden surface profile and radial gas velocity distribution were made using an air-flow indicator. Upon the completion of charging, a coaxial, semicircular metal frame dividing the furnace cross section into eight equal parts was driven into the charge layer so that size analysis samples could be collected.

### 3.4 Experimental Results of the Trajectory of Falling Burden

**Figure 5** shows the main flow trajectories of the falling burden and their final positions at respective angles of the distributing chute of inclination and stock-lines SL (corresponding to 0, 0.5 and 1 m). Trajectories were similar for cokes and ores.

**Figure 6** shows a comparison between the flow-out velocity of the burden at the chute tip obtained in the model experiment, corrected for the scale of reduction, and that for a PW type used in the actual furnace. Flow-out velocity is dependent on the angle of inclination of the distribution chute. The velocity is higher with the Cardan type than with the PW type, and the trajectory lies nearer the periphery.

**Figure 7** shows a comparison of the relation between the angle of inclination of the distribution chute and the

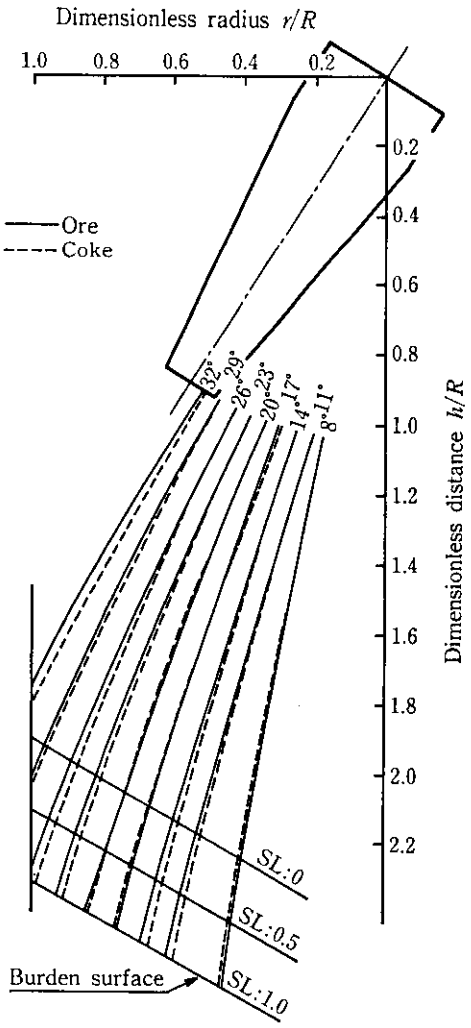


Fig. 5 Falling trajectory of main flow

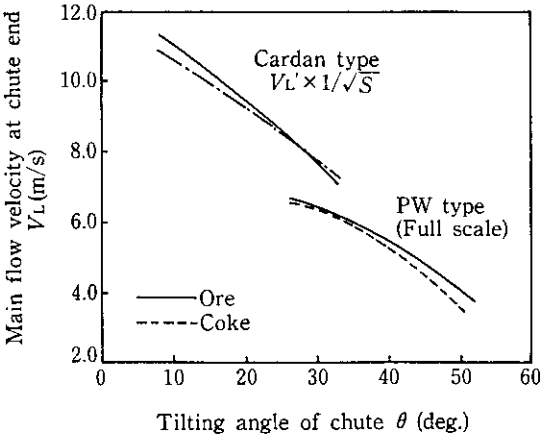


Fig. 6 Relationship between main flow velocity and tilting angle of chute

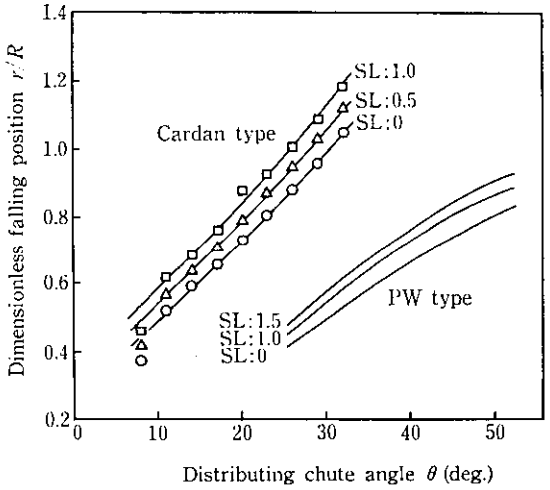


Fig. 7 Relationship between chute angle and falling position of burden (ore)

principal final position of the burden in the two types. Compared with the PW type, the Cardan type has a smaller angle of inclination, and yet the burden falls at the same position as with the PW type. This is due to the higher burden flow-out velocity in the Cardan type and to the greater length of the distribution chute with respect to the furnace throat radius.

### 3.5 Selection of Distributing Chute Angle of Inclination for Actual Furnace

In our Cardan type charging apparatus, the available range of distribution chute inclination angles is 0 to 36°. The fixed angles of distribution chute inclination in the ferromanganese smelting furnace were selected within the range of 8 to 26° on the basis of the following conditions, in order to obtain a proper burden distribution.

(1) Decreased wear of the furnace wall is desirable.
(2) The angle of inclination should be one whereby the main flow of the burden will fall at the same position as in the PW type.
(3) Ten points should be selected so that the burden material falling during one chute turn will cover equal cross sectional areas of the burden surface.

### 3.6 Features of Burden Distribution with Cardan Type Charging Apparatus

To determine the features of burden distribution with the Cardan type, and of optimum burden distribution, a charging test was conducted under the conditions shown in Table 1.

In **Fig. 8**, a burden distribution with the Cardan device is shown in comparison with a case with the PW-type model experiment. The charging pattern was set to

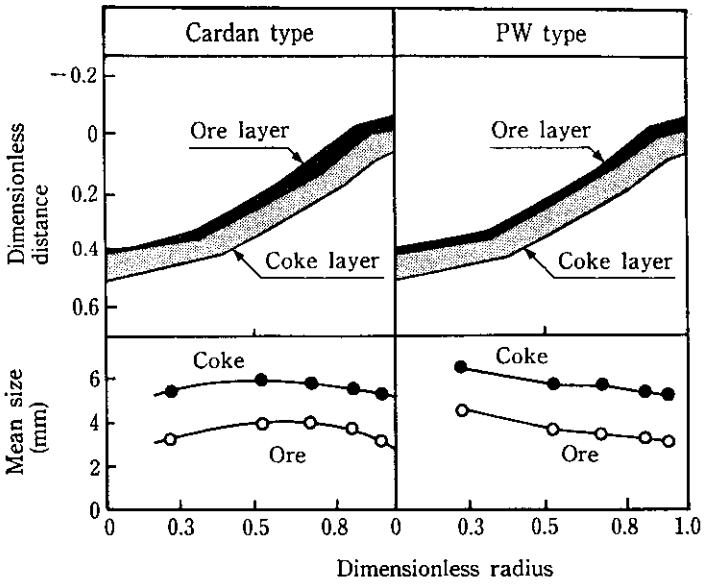


Fig. 8 Distribution of burden materials at furnace top

be similar, in terms of burden falling position, to the pattern in high-coke-rate operation at No. 6 blast furnace of Chiba Works, which is equipped with a PW bell-less charging apparatus. From the burden profile in Fig. 8, it was found that ore in the Cardan type is not charged at the center, which indicates that the flow-in of ore in the central direction was slight, in spite of the fact that the burden with the Cardan type was charged at the same position as with the PW type. In addition, the particle size distributions of coke and ore in the radial direction with the Cardan type were greater at the middle area and smaller at the center and periphery. This was because the angle of inclination of the rotary chute was controlled so that the burden would be charged from the periphery toward the furnace center during the period from the start of charging till its end, and time dependent changes in particle size in the hopper discharge shown in **Fig. 9** appeared as a radial direction distribution. It is a feature of the Cardan type that since burden flow-in in the central direction is low, size segregation[4] due to flow-in was also slight. Thus, particle size distribution in the radical direction is mainly related to particle size behavior at the time of hopper discharge. Flow-in is low, as shown in **Table 2**, because the velocity ratio, $V_X/V_Y$ (horizontal velocity component/vertical velocity component), at which the burden collides with the charged surface with the Cardan type is greater than with the PW type. It is surmised that since the velocity component in the periphery direction with the Cardan type is greater, the flow-in in the furnace center direction, which is the reverse direction, is suppressed.

Burden profile, layer thickness distribution, and gas

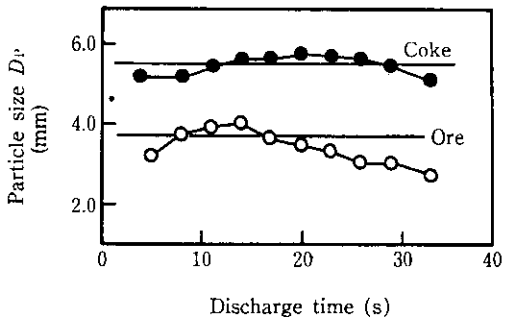


Fig. 9 Transition of particle size in discharge from hopper

Table 2 Comparison of the ratios of $V_X/V_Y$ between Cardan type and PW type

| | Cardan type | | | PW type | | | |
|---|---|---|---|---|---|---|---|
| Tilting position | 1 | 6 | 9 | 1 | 6 | 9 | 10 |
| Tilting angle (°) | 26.0 | 19.7 | 13.7 | 52.0 | 41.5 | 31.5 | 25.5 |
| $V_X/V_Y$ | 0.952 | 1.139 | 1.272 | 0.255 | 0.433 | 0.591 | 0.666 |

flow velocity distribution are shown in **Fig. 10** for various charging patterns with the Cardan type. To obtain a uniform distribution of the ore layer thickness with the Cardan type, a pattern in which ore can be charged up to the central area is necessary. In the conventional PW type, the gas velocity distribution at the center increases sharply, while with the Cardan type, particle segregation is minimal and the ore layer is thin, causing a gently sloped velocity distribution.

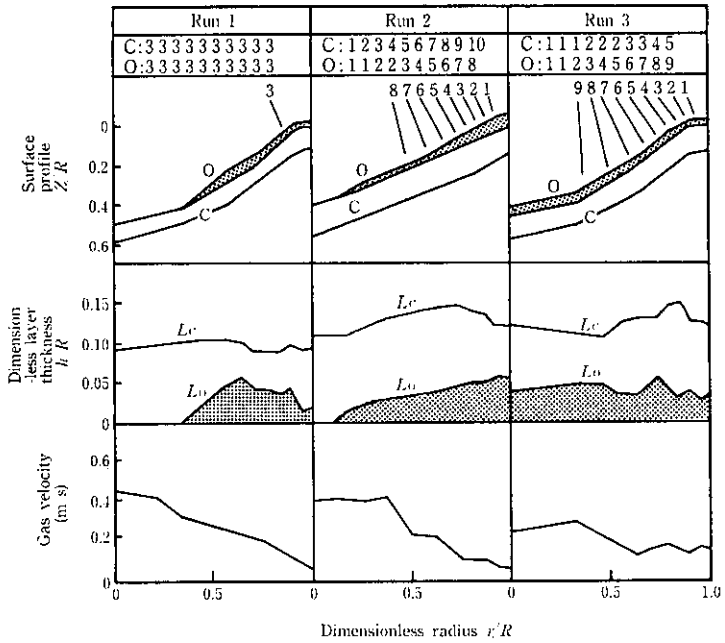


Fig. 10 Distribution of burden materials at furnace top (SL = 0.5)

## 4 Filling Test

### 4.1 Burden Distribution in Radial Direction

The methods of measuring the trajectory of falling burden, the burden profile, and particle size distribution were the same as those in a previous report.[5] As an additional consideration, changes in particle size during the discharge of material from the hopper were also investigated. To achieve this, at every turn of the distribution chute, the burden was sampled from the burden-top manhole, and a particle size analysis was made.

The trajectory of falling materials is shown in **Fig. 11**, the particle size distribution in the radial direction in **Fig. 12**, and changes in particle size during discharge from the hopper in **Fig. 13**. These results agreed well with those of the model experiment, confirming the predicted burden distribution characteristics of the Cardan type charging apparatus.

### 4.2 Burden Distribution in Circumferential Direction

It is important that, as much as possible, control of burden distribution be uniform in the circumferential direction, as in the radial direction. Non-uniformity of distribution in the circumferential direction is largely attributable to the construction of the charging apparatus. With bell-type blast furnace tops, for instance, circumferential imbalance is probably caused by the directionality of the charging belt conveyor (B.C.). The PW-type bell-less apparatus of the parallel hopper type poses a different problem: Since the burden-top hopper

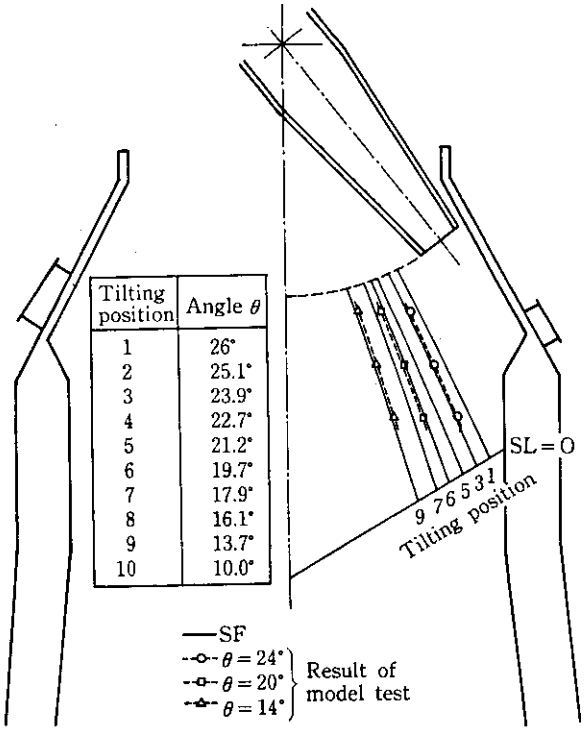


Fig. 11 Falling trajectory of materials in actual furnace at filling

was not located on the central axis of the blast furnace, burden flow and particle size segregation developed directionality, disturbing the circumferential balance.[6] Therefore, an investigation was made of circumferential

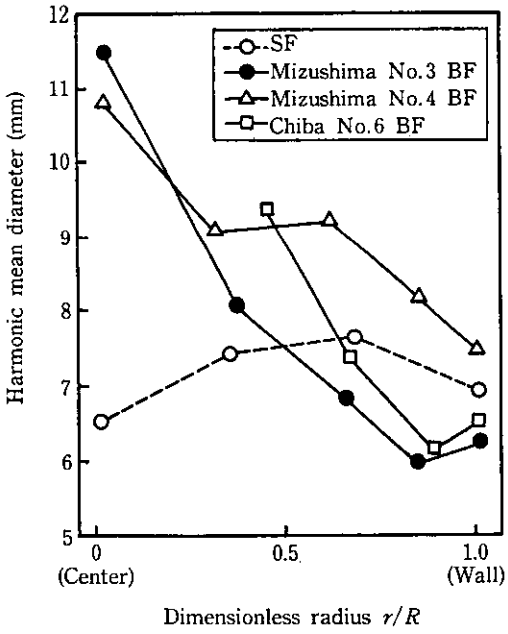


Fig. 12 Size distribution of burden materials

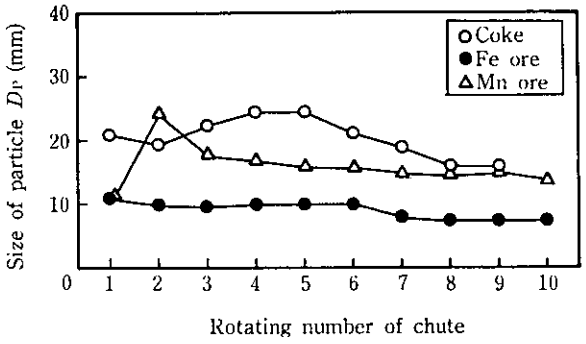


Fig. 13 Transition of particle size in discharge from upper hopper

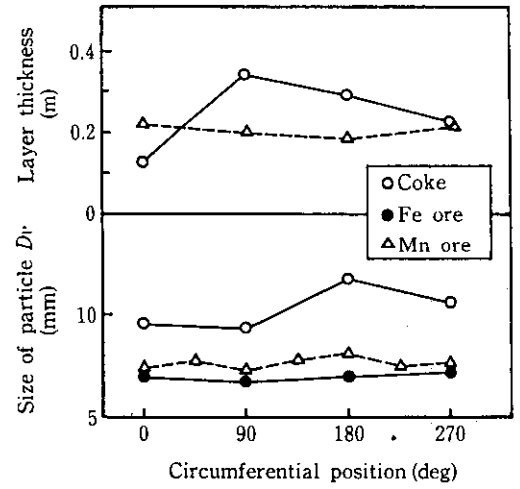


Fig. 14 Circumferential distribution of layer thickness and particle size

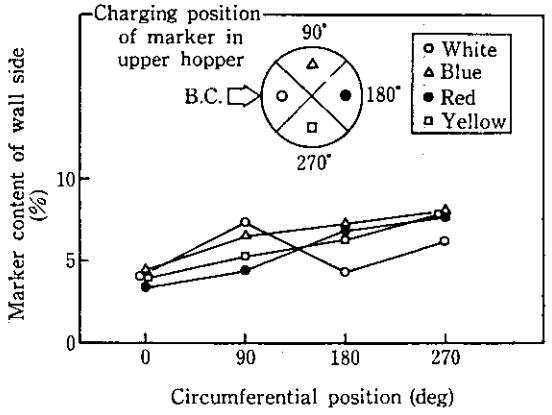


Fig. 15 Circumferential distribution of marker content

balance with the Cardan device equipped with 2-stage hoppers on the same central axis as that of the furnace.

Layer thickness deviation and particle-size deviation at the periphery are shown in **Fig. 14**. The Cardan type shows minimal deviation in the circumferential direction and a uniform distribution. Equal quantities of four colored ores were charged into the upper hopper, and the distribution of the respective ores in the circumferential direction at the periphery of the burden top was investigated. The results are shown in **Fig. 15**. The respective colored ores charged into the furnace through the upper hopper, lower hopper, and distribution chute were well mixed and uniformly distributed at the burden top, in spite of being charged separately at different positions in the upper hopper.

## 5 Progress of Actual Operation

The ferromanganese smelting furnace was blown in on June 24, 1985. The progress of the start-up operation is shown in **Fig. 16**, and changes in selected charging patterns in **Fig. 17**. In the initial stage of start-up, ore was charged according to a charging pattern based on results of the model experiment. This pattern produced a uniform layer thickness distribution in the radial direction and resulted in trouble-free operation. However, when the increased-production operation began in September, it was found that the charging pattern used in initial operation caused an increase in periphery heat loss and somewhat poorer burden descent, and a charging pattern of the central gas flow type, similar to run 2 in Fig.

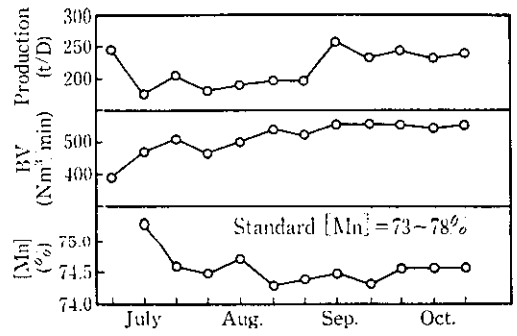


Fig. 16 Operation data of Fe-Mn smelting furnace

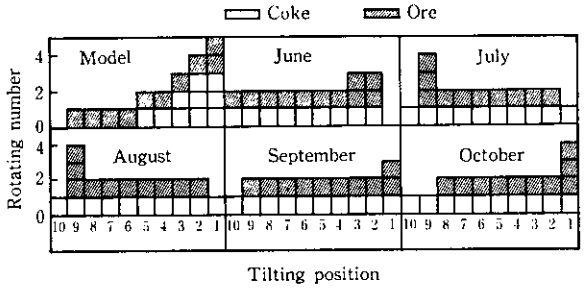


Fig. 17 Typical charging pattern

10 of the model experiment, was adopted. Since then, fluctuations in product ingredients have decreased and operation is now stable.

## 6 Conclusions

A center-feed Cardan type bell-less top was adopted with the ferromanganese smelting furnace to achieve stabilization of ferromanganese manufacturing by means of burden distribution control and to cope with the high temperature of the furnace top gas. Prior to the introduction of the Cardan apparatus, the device's burden distribution characteristics were investigated using a small scale model. The proper angle of inclination of the distribution chute during the smelting furnace operation was selected after examining the similarity conditions between the model experiment and actual operation, and the burden distribution characteristics of the charging apparatus were clarified. Further, the results of the investigation at the time of filling were collated with those of the model experiment. Results obtained were as follows:

(1) In the model experment, a model apparatus with $S = 1/7.5$ was used; it was found that the similarity conditions between the model and the actual furnace were satisfied by the following equations:

$$\frac{\omega^*}{\omega} = \sqrt{\frac{L}{L^*}} = \frac{1}{\sqrt{S}}, \quad \frac{V_0^*}{V_0} = \sqrt{\frac{L^*}{L}} = \sqrt{S}$$

(2) The optimum angle of inclination of the distribution chute of the actual furnace is within 8 to 26°C.

(3) The radial direction velocity component of particles at the tip of the distribution chute in the Cardan type was greater than that of the PW type. Therefore, with the Cardan type, the burden can be charged to a wider range of positions in the furnace using a smaller distribution chute angle.

(4) With the Cardan type, the flow-in of the burden in the direction of the furnace center and particle segregation were less. Also, in the center-feed type, deviation of burden distribution in the circumferential direction at the burden top was less.

(5) A burden distribution survey in the smelting furnace at the time of filling disclosed that distribution characteristics showed good agreement with results of the model experiment. Layer thickness and particle size deviation in the circumferential direction were less, indicating a more uniform distribution.

(6) Results of the model experiment and the actual furnace survey at filling were applied to the smelting furnace operation and contributed to a successful start-up and subsequent stable operation.

### References


1) K. Yoshida, Y. Serizawa, H. Kokubu, S. Suzuki, M. Masukawa, and H. Itaya: *Kawasaki Steel Giho*, **19**(1987)2, 73
2) T. Nasu: *Ishikawajima-Harima Engineering Review*, **26**(1986)1, 56
3) M. Kondo, K. Okabe, J. Kurihara, K. Okumura, and S. Tomita: *Tetsu-to-Hagané*, **63**(1977)11, S441
4) S. Miwa: "Fun-Ryutai Kogaku (Particulate Technology)," (1972) p. 221, [Asakura Shoten]
5) T. Yamada, M. Satou, S. Miyazaki, T. Simamura, and S. Taguchi: *Kawasaki Steel Giho*, **6**(1974)1, 16
6) S. Nomura, S. Taguchi, N. Tuchiya, A. Katou, K. Tanaka, and K. Okumura: *Tetsu-to-Hagané*, **68**(1982)11, S702